

# Accepted Manuscript

Synthesis and evaluation of novel dual BRD4/HDAC inhibitors

Seika Amemiya, Takao Yamaguchi, Yuichi Hashimoto, Tomomi Noguchi-Yachide

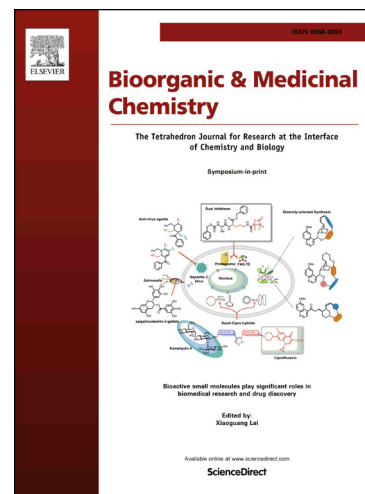
PII: S0968-0896(17)30764-2  
DOI: <http://dx.doi.org/10.1016/j.bmc.2017.04.043>  
Reference: BMC 13713

To appear in: *Bioorganic & Medicinal Chemistry*

Received Date: 7 April 2017  
Accepted Date: 28 April 2017

Please cite this article as: Amemiya, S., Yamaguchi, T., Hashimoto, Y., Noguchi-Yachide, T., Synthesis and evaluation of novel dual BRD4/HDAC inhibitors, *Bioorganic & Medicinal Chemistry* (2017), doi: <http://dx.doi.org/10.1016/j.bmc.2017.04.043>

This is a PDF file of an unedited manuscript that has been accepted for publication. As a service to our customers we are providing this early version of the manuscript. The manuscript will undergo copyediting, typesetting, and review of the resulting proof before it is published in its final form. Please note that during the production process errors may be discovered which could affect the content, and all legal disclaimers that apply to the journal pertain.



Synthesis and evaluation of novel dual BRD4/HDAC inhibitors

Seika Amemiya, Takao Yamaguchi, Yuichi Hashimoto, Tomomi  
Noguchi-Yachide\*

Institute of Molecular and Cellular, Biosciences, the University of Tokyo, 1-1-1 Yayoi,  
Bunkyo-ku, Tokyo 113-0032, Japan

\* Corresponding author.

T. Noguchi-Yachide

Institute of Molecular & Cellular Biosciences, The University of Tokyo

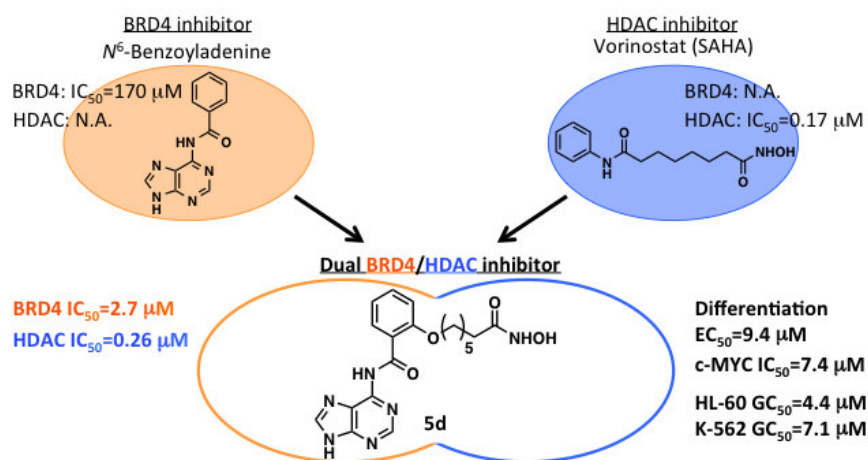
1-1-1 Yayoi, Bunkyo-ku, Tokyo 113-0032, Japan

E-mail: [noguchi@iam.u-tokyo.ac.jp](mailto:noguchi@iam.u-tokyo.ac.jp)

Tel: +81.3.5841.7875

Fax: +81.3.5841.8495

**Graphical abstract**



**Keywords:** BET bromodomain; BRD4; HDAC; Benzoyladenine; Structure-activity relationship; Polypharmacology

### Abstract

Epigenetic regulation of gene expression via histone acetylation modulates many cellular processes, including apoptosis, the cell cycle, cell growth and differentiation, and inhibitors are promising drug candidates. We have previously developed inhibitors of BRD4, which recognizes acetylated lysine residue on histones and recruits transcription elongation factor to the transcription start site, while inhibitors of histone deacetylase (HDAC), which catalyzes the removal of acetyl groups on histones, are already in clinical use for cancer treatment. Based on the idea that polypharmacological agents with multiple targets would have a more robust action, we set out to develop dual BRD4/HDAC inhibitors. Here, we describe the design and synthesis of N<sup>6</sup>-[2-(7-hydroxyamino-7-oxoheptyloxy)benzoyl]adenine (**5d**) as a BRD4/HDAC dual inhibitor. This compound showed HL-60 cell growth-inhibitory and apoptosis-inducing activity, as well as all-*trans* retinoic acid (ATRA)-induced HL-60 cell differentiation-enhancing activity, and c-MYC production-inhibitory activity.

Interestingly, it also showed growth-inhibitory activity towards BRD4 inhibitor-resistant cells.

## 1. Introduction

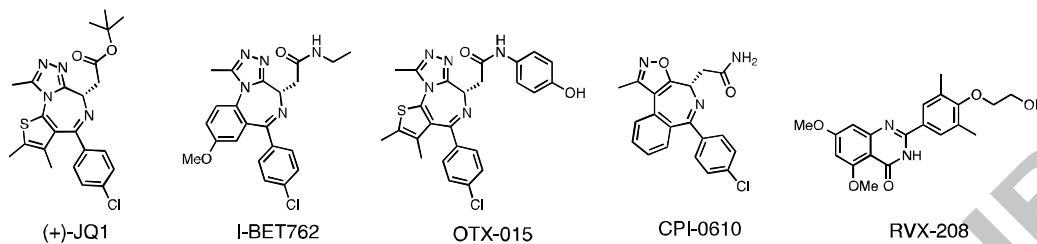
Polypharmacology has been receiving increasing attention as a novel strategy in drug development over the past decade. In contrast to the conventional one-drug/one-target philosophy,<sup>1, 2)</sup> polypharmacology aims to develop drugs with multiple related targets in order to obtain more robust effects on diseases involving dysfunction of complex biological networks, such as cancers and inflammatory diseases. This approach addresses some of the issues that can occur with multidrug chemotherapy (polypharmacy), such as drug-drug interaction and poor medication compliance.<sup>3)</sup>

We have previously developed BRD4 inhibitors and reported their structure-activity relationships.<sup>4, 5)</sup> BRD4 is the most extensively studied member of the bromodomain and extra-terminal domain (BET) family proteins, which consist of BRD2, BRD3, BRD4 and BRDT. BRD4 recognizes acetylated lysine residue (Kac) on histones *via* its tandem *N*-terminal bromodomains and also interacts with positive transcription elongation factor b (P-TEFb), a heterodimer of cyclin-dependent kinase 9 (CDK9) and its regulator cyclin T, through its *C*-terminal domain.<sup>6, 7)</sup> BRD4 recruits P-TEFb to the transcription start site, leading to transcription elongation through phosphorylation of the carboxyl-terminal of RNA polymerase II.<sup>8)</sup> Moreover, BRD4 can act as a super-enhancer, driving expression of oncogenes, such as the *c-MYC* oncogene, in tumor cells and facilitating transcription.<sup>9)</sup> In addition, BRD4 was recently reported to promote elongation of noncoding enhancer RNAs (eRNAs), in a manner dependent on interaction between the bromodomain and Kac on histones.<sup>10)</sup> Thus, BRD4 is involved in modulation of a wide range of biological functions that are potentially relevant to the treatment of cancers, including apoptosis, the cell cycle, growth, proliferation, differentiation and invasion. Consequently, BET bromodomains are promising therapeutic targets for cancers, and many BET inhibitors with Kac-mimetic moieties (Fig. 1), including (+)-JQ1, I-BET762, OTX-015, CPI-0610, RVX-208, have been reported since the first inhibitor was developed in 2010.<sup>11)</sup> Some of them are in clinical trials for the treatment of cancers such as multiple myeloma (MM) and nuclear protein in testis (NUT) midline carcinoma (NMC).<sup>12, 13)</sup>

On the other hand, histone deacetylases (HDACs) are involved in regulating histone acetylation. The HDAC superfamily consists of eleven zinc-containing amidehydrolases, which are classified into four major classes (class I, IIa, IIb and IV), and seven sirtuins (SIRT1-7), which are referred to as class III and are NAD-dependent amidehydrolases. By removing acetyl groups on histones, HDACs play key roles in the epigenetic regulation of gene expression, modulating many cellular processes, including apoptosis, the cell cycle, growth and differentiation.<sup>14, 15)</sup> In acute promyelocytic leukaemia (APL) and acute myeloid leukaemia (AML), HDACs are aberrantly recruited to promoters through physical association with oncogenic DNA-binding fusion proteins and HDAC-containing repressor complexes, resulting in repression of specific target genes.<sup>16-18)</sup> Numerous HDAC inhibitors have been reported (Fig. 1) as candidate drugs in the field of oncology. Among them, vorinostat (SAHA; Fig. 1) was approved by the U.S. Food and Drug Administration (FDA) for the treatment of the cutaneous manifestations of cutaneous T cell lymphoma (CTCL).<sup>19)</sup>

Since both BRD4 and HDAC are related to epigenetic regulation of gene expression via histone acetylation, and are associated with similar biological phenotypes related to cancer,<sup>20)</sup> there is a great interest in developing dual BRD4/HDAC inhibitors. Here, we report the design and synthesis of dual BRD4/HDAC inhibitors. We also examined their effects on cancer cells in order to assess their potential utility as candidate polypharmacological drugs for treatment of cancer.

## A) BET inhibitors



## B) HDAC inhibitors

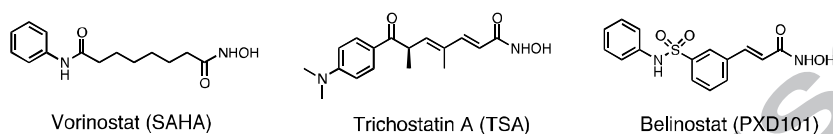
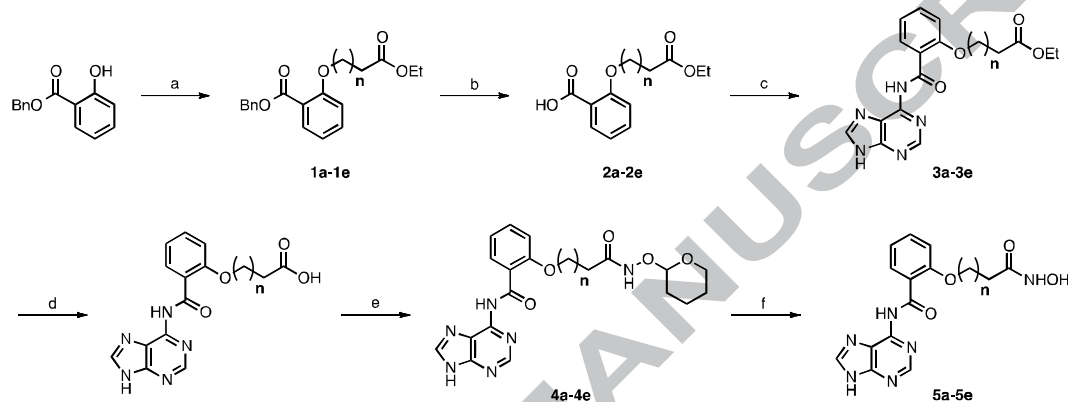


**Figure 1.** Chemical structures of typical BET and HDAC inhibitors

## 2. Results and discussion

We have reported  $N^6$ -benzoyladenine as a new chemical scaffold for development of BRD4 inhibitors and examined its structure-activity relationship (SAR).<sup>4, 5)</sup> Subsequently, related BET bromodomain inhibitors with a  $9H$ -purine moiety were reported to interact with the conserved asparagine (Asn140) in the Kac-binding pocket of BRD4 *via* purine nitrogen.<sup>21)</sup> Thus, we considered that the  $N^6$ -benzoyladenine moiety serves as a mimic of Kac. In our previous work, we found that compounds with an electron-donating substituent at the 2-position of the benzoyl group possess more potent BRD4-inhibitory activity than those with an electron-accepting substituent, and  $N^6$ -(2-phenoxybenzoyl)adenine and  $N^6$ -(2-pentyloxybenzoyl)adenine (**6**) retained the inhibitory activity.<sup>4, 5)</sup> These observations imply that there is unoccupied space between the 2-position of the benzoyl group of  $N^6$ -benzoyladenine derivatives and BRD4 in the Kac-binding pocket. On the other hand, the SAR of HDACs has been extensively studied. Many HDAC inhibitors consist of a zinc-binding group, which chelates the zinc ion at the bottom of the HDAC active site, such as a hydroxamic group coupled *via* a spacer moiety to a cap group, which occupies a position between the hydrophobic residues at the entrance of the HDAC active site.<sup>22)</sup> Based on these findings, we designed and synthesized **5a-5e** as candidate dual BRD4/HDAC inhibitors (Scheme 1). These compounds, in which  $N^6$ -benzoyladenine as a BRD4-binding moiety is connected to a hydroxamic group as an HDAC-binding moiety by a flexible alkyl linker, were prepared

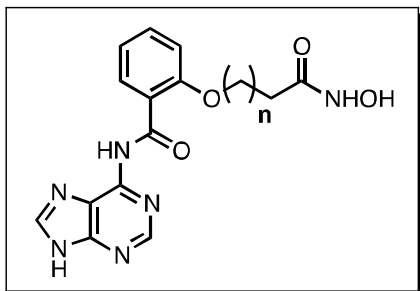
as shown in Scheme 1. Briefly, benzyl 2-hydroxybenzoates were alkylated to afford **1a-1e**. Deprotection of the benzyl group afforded **2a-2e**, which were condensed with adenine in DMA to give **3a-3e**. After de-esterification of **3a-3e**, the compounds were condensed with THP-protected hydroxylamine to afford **4a-4e**. Deprotection of the THP group gave the desired compounds **5a-5e**.



**Scheme 1.** Synthesis of compounds **5a-5e**. Reaction conditions: (a) alkyl bromide,  $K_2CO_3$ , MeCN, 54%-quant.; (b)  $H_2$ , Pd/C, EtOH, 64-99%; (c) adenine, EDCI·HCl, DMA, 5-25%; (d)  $LiOH \cdot H_2O$ , THF,  $H_2O$ ; (e)  $NH_2OTHP$ ,  $HOBT \cdot H_2O$ , EDCI·HCl, DMF, 20-87% (2 steps); (f)  $p$ -TsOH· $H_2O$ , MeOH, 24-81%.

The BRD4- and HDAC-inhibitory activities of these compounds were investigated using commercially available assay kits, BRD4 bromodomain 1 TR-FRET assay kit (Cayman) and *Fluor de Lys®-Green* HDAC Assay kit (Enzo Life Sciences). (+)-JQ1, which is a pan-BET bromodomain inhibitor, and vorinostat, which is a pan-HDAC inhibitor, were used as positive controls. Compounds **5a-5e**, which were prepared to evaluate the influence of linker length, showed both BRD4- and HDAC-inhibitory activities (Table 1). Among them, **5d** with a hexyl linker exhibited the most potent BRD4/HDAC dual-inhibitory activities.

**Table 1.** BRD4- and HDAC-inhibitory activities of **5a-5e**.



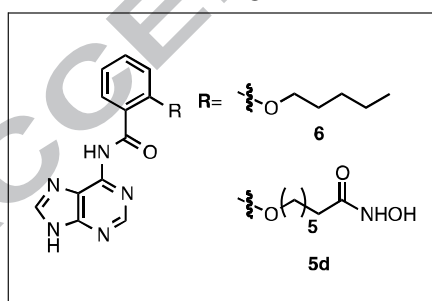
compound	n	BRD4 IC <sub>50</sub> (μM)	HDAC IC <sub>50</sub> (μM)
(+)-JQ1	-	0.82	N.A. <sup>a</sup>
vorinostat	-	N.A. <sup>a</sup>	0.17
<b>5a</b>	2	25	29
<b>5b</b>	3	7.4	12
<b>5c</b>	4	3.8	2.6
<b>5d</b>	5	2.7	0.26
<b>5e</b>	6	7.4	0.53

<sup>a</sup> N.A. = no activity at 100 μM

Next, we investigated the cell growth-inhibitory activity, all-*trans* retinoic acid (ATRA)-induced cell differentiation-enhancing activity, and c-MYC production-inhibitory activity in order to evaluate the potential of **5d** as an anti-cancer agent.<sup>23-31</sup> In addition, we evaluated the suitability of **5d** for polypharmacology by using BRD4 inhibitor-resistant cells.

Firstly, we investigated the growth-inhibitory activity of **5d** towards a human promyelocytic leukemia cell line, HL-60, in comparison with *N*<sup>6</sup>-(2-pentyloxybenzoyl)adenine (**6**), which we have previously reported as a BRD4 inhibitor.<sup>5</sup> As shown in Table 2, (+) JQ1, vorinostat, **6**, and **5d** all showed HL-60 cell growth-inhibitory activity. The activities decreased in the following order: (+)-JQ1 > vorinostat > **6** > **5d**.

**Table 2.** HL-60 cell growth-inhibitory activity and differentiation-inducing activity



compound	HL-60 GC <sub>50</sub> (μM)	Differentiation EC <sub>50</sub> (μM)	BRD4 IC <sub>50</sub> (μM)	HDAC IC <sub>50</sub> (μM)
(+)-JQ1	0.060	0.20	0.82	N.A. <sup>a</sup>
vorinostat	0.39	1.3	N.A. <sup>a</sup>	0.17
<b>6</b>	1.6	5.9	7.1	N.A. <sup>a</sup>
<b>5d</b>	4.4	9.4	2.7	0.26

<sup>a</sup> N.A. = no activity at 100 μM

Next, we also examined whether **5d** induces apoptosis. We double-stained HL-60 cells with Annexin V-FITC and PI, and detected apoptotic cells using flow cytometry. Annexin

V-positive cells increased after incubation with **5d** for 24 h, and **5d** showed time-dependent apoptosis-inducing activity (Fig. 2D-F). We confirmed the expression of cleaved caspase 3 and cleaved poly ADP-ribose polymerase (PARP) as indicators of apoptosis by western blot analysis. Compounds **6** and **5d** both showed time-dependent cleavage of caspase 3 and PARP (Figure 3). Overall, the results of flow cytometry and western blot analysis indicated that **6** and **5d** cause growth inhibition followed by apoptosis.

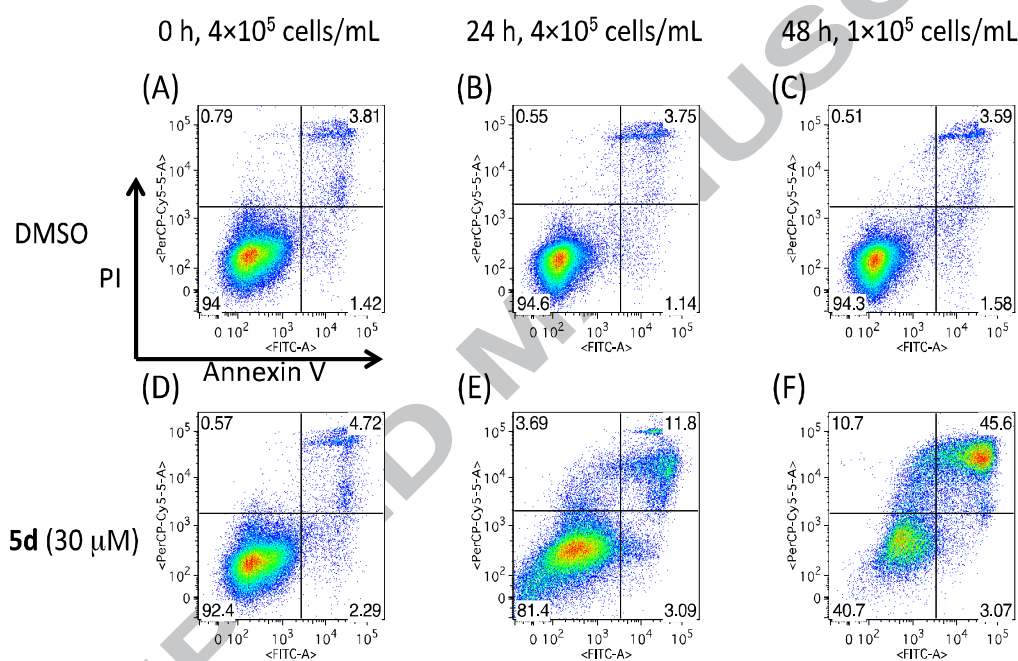


**Figure 2.** Detection of apoptotic cells by Annexin V and PI double staining

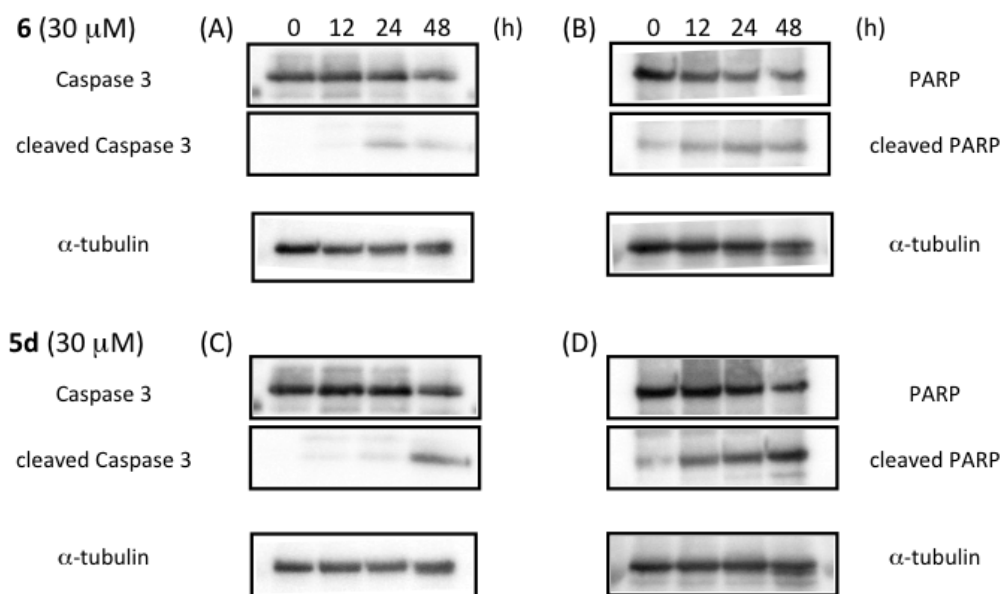
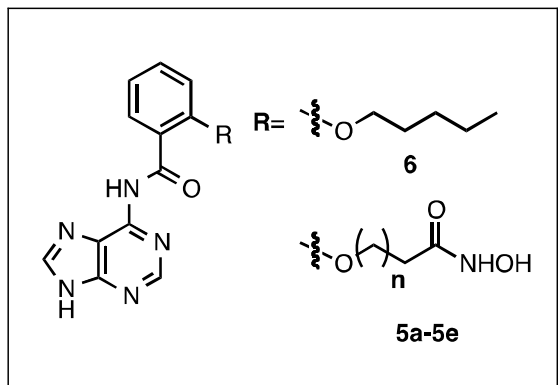


**Figure 3.** Western blot analysis of caspase 3 and PARP

Secondly, we investigated the effect of **5d** on ATRA-induced HL-60 cell differentiation. ATRA was selected because it is used in differentiation therapy for APL, and is an endogenous active form of vitamin A that is generally present in normal serum. HL-60 cells were incubated in the presence of test compound with 0.6 nM ATRA, which is approximately equal to the endogenous retinoic acid concentration in human plasma. (+)-JQ1, vorinostat, **6**, and **5d** all enhanced ATRA-induced cell differentiation, and the activities decreased in the following order: (+)-JQ1 > vorinostat > **6** > **5d** (Table 2).

Thirdly, we investigated c-MYC production-inhibitory activity. As shown in Table 3, (+)-JQ1, vorinostat, **6**, **5d**, and **5e** showed c-MYC production-inhibitory activity, while **5a-5c** did not. The activities decreased in the following order: (+)-JQ1 > vorinostat > **6** > **5e** > **5d**. The reason why **5a-5c** were inactive may be that these compounds have low permeability across the cell membrane. Overall, the results in Fig. 2, Fig. 3, and Table 2 suggest that dual BRD4/HDAC inhibitor **5d** is a promising candidate agent for treatment of cancer.

**Table 3.** c-MYC production-inhibitory activity



compound	n	c-MYC IC <sub>50</sub> (μM)
(+)-JQ1	-	0.086-0.093
vorinostat	-	0.74
<b>6</b>	-	2.2-2.4
<b>5a</b>	2	N.A. <sup>a</sup>
<b>5b</b>	3	N.A. <sup>a</sup>
<b>5c</b>	4	N.A. <sup>a</sup>
<b>5d</b>	5	7.4-8.0
<b>5e</b>	6	5.7-7.3

<sup>a</sup> N.A. = no activity at 100 μM

Finally, we evaluated the growth-inhibitory effect of **5d** on K-562, T-47D, and OVCAR-5 cell lines, which are (+)-JQ1-resistant, and on HL-60, MCF-7, MDA-MB-231, and A2780 cell lines, which are (+)-JQ1-sensitive.<sup>25, 32-34</sup> As shown in Table 4, (+)-JQ1 and **6** showed weaker growth-inhibitory activity towards leukemia K-562 cells compared with leukemia HL-60 cells, while vorinostat and **5d** showed equivalent activities towards both K-562 and HL-60 cells. Similar results were observed with ovarian cancer cells, OVCAR-5 cells and A2780 cells. On the other hand, **5d** showed weaker activity in breast cancer cells, MCF-7 cells and MDA-MB-231 cells, but showed comparable activity to (+)-JQ1 in T-47D cells. Thus, **5d** is effective against BRD4 inhibitor-resistant cells.

**Table 4.** Growth-inhibitory activities towards various cancer cell lines

compound	leukemia cells		breast cancer cells			ovarian cancer cells	
	HL-60 GC <sub>50</sub> (μM)	K-562 GC <sub>50</sub> (μM)	MCF-7 GC <sub>50</sub> (μM)	MDA-MB-231 GC <sub>50</sub> (μM)	T-47D GC <sub>50</sub> (μM)	A2780 GC <sub>50</sub> (μM)	OVCAR-5 GC <sub>50</sub> (μM)
(+)-JQ1	0.060	3.8	1.7	0.30	2.8	4.0	12
vorinostat	0.39	0.80	4.6	2.7	1.4	1.0	0.99
<b>6</b>	1.6	12	23	11	9.0	21	29
<b>5d</b>	4.4	7.1	34	10	2.3	14	18

### 3. Conclusion

We designed and synthesized novel dual BRD4/HDAC inhibitors **5a-5e** based on the structure-activity relationships of *N*<sup>6</sup>-benzoyladenine derivatives. Among these compounds, **5d** showed the most potent BRD4/HDAC dual-inhibitory activities, and also possessed HL-60 cell growth-inhibitory activity, HL-60 cell differentiation-inducing

activity, and c-MYC production-inhibitory activity. Moreover, it showed a significant growth-inhibitory effect on BRD4-resistant cells. These results suggest that polypharmacology may be an effective strategy for the treatment of cancers.

## 4. Experimental Section

### 4.1. General chemistry

<sup>1</sup>H-NMR spectra were recorded on a JEOL JNM-ECA-500 (500 MHz) spectrometer. Chemical shift values were expressed in  $\delta$  values (ppm) relative to internal tetramethylsilane (0.00 ppm), residual CHCl<sub>3</sub> (7.26 ppm), CHD<sub>2</sub>OD (3.31 ppm), or C<sub>2</sub>HD<sub>5</sub>SO (2.49 ppm) for <sup>1</sup>H-NMR, and internal tetramethylsilane (0.00 ppm), chloroform-*d*<sub>1</sub> (77.16 ppm), methanol-*d*<sub>4</sub> (49.00 ppm), or dimethylsulfoxide-*d*<sub>6</sub> (39.50 ppm) for <sup>13</sup>C-NMR. Electrospray ionization (ESI) and fast atom bombardment (FAB) mass spectra were recorded on a Bruker micrOTOF II mass spectrometer. Melting points were determined by using a MP-J3 melting point apparatus (Yanako). Thin layer chromatography (TLC) was performed on silica gel 60 F254 plates (Merck). Flash column chromatography was performed on silica gel 60 (spherical, particle size 40-100  $\mu$ m; Kanto).

#### 4.1.1. Synthesis

##### *General synthetic procedure for benzyl 2-(ethoxy-oxoalkoxy)benzoates*

The corresponding alkyl bromide (2.0 eq) and potassium carbonate (2.0 eq) were added to a solution of benzyl 2-hydroxybenzoate (1.0 eq) in CH<sub>3</sub>CN, and the mixture was refluxed. After completion of the reaction, the residue was purified by silica gel column chromatography (EtOAc/Hexane) to afford the product.

##### 4.1.1.1. Benzyl 2-(4-ethoxy-4-oxobutyloxy)benzoate (1a)

Colorless oil (quant.): <sup>1</sup>H-NMR (500 MHz, CDCl<sub>3</sub>)  $\delta$  1.24 (t, *J*=6.9 Hz, 3H), 2.05-2.11 (m, 2H), 2.47 (t, *J*=7.5 Hz, 2H), 4.07 (t, *J*=6.3 Hz, 2H), 4.12 (q, *J*=7.5 Hz, 2H), 5.34 (s, 2H), 6.93-6.97 (m, 2H), 7.30-7.33 (m, 1H), 7.35-7.38 (m, 2H), 7.41-7.46 (m, 3H), 7.82 (d, *J*=7.5 Hz, 1H); ESI-TOF-HRMS (M+Na)<sup>+</sup> calculated for C<sub>20</sub>H<sub>22</sub>O<sub>5</sub>Na 365.1359; found 365.1373.

**4.1.1.2. Benzyl 2-(5-ethoxy-5-oxopentyloxy)benzoate (1b)**

Colorless oil (94 %):  $^1\text{H-NMR}$  (500 MHz,  $\text{CDCl}_3$ )  $\delta$  1.24 (t,  $J=6.9$  Hz, 3H), 1.72-1.85 (m, 4H), 2.30 (t,  $J=7.5$  Hz, 2H), 4.02 (t,  $J=6.3$  Hz, 2H), 4.11 (q,  $J=7.5$  Hz, 2H), 5.34 (s, 2H), 6.92-6.97 (m, 2H), 7.32-7.38 (m, 3H), 7.41-7.45 (m, 3H), 7.82 (d,  $J=7.5$  Hz, 1H); ESI-TOF-HRMS ( $\text{M}+\text{Na}$ ) $^+$  calculated for  $\text{C}_{21}\text{H}_{24}\text{O}_5\text{Na}$  379.1516; found 379.1499.

**4.1.1.3. Benzyl 2-(6-ethoxy-6-oxohexyloxy)benzoate (1c)**

Colorless oil (86 %):  $^1\text{H-NMR}$  (500 MHz,  $\text{CDCl}_3$ )  $\delta$  1.25 (t,  $J=6.9$  Hz, 3H), 1.42-1.48 (m, 2H), 1.60-1.66 (m, 2H), 1.75-1.81 (m, 2H), 2.26 (t,  $J=8.0$  Hz, 2H), 4.00 (t,  $J=6.3$  Hz, 2H), 4.12 (q,  $J=7.5$  Hz, 2H), 5.34 (s, 2H), 6.92-6.96 (m, 2H), 7.30-7.33 (m, 1H), 7.35-7.38 (m, 2H), 7.40-7.45 (m, 3H), 7.81 (d,  $J=7.5$  Hz, 1H); ESI-TOF-HRMS ( $\text{M}+\text{Na}$ ) $^+$  calculated for  $\text{C}_{22}\text{H}_{26}\text{O}_5\text{Na}$  393.1672; found 393.1698.

**4.1.1.4. Benzyl 2-(7-ethoxy-7-oxoheptyloxy)benzoate (1d)**

Colorless oil (quant.):  $^1\text{H-NMR}$  (500 MHz,  $\text{CDCl}_3$ )  $\delta$  1.24 (t,  $J=6.9$  Hz, 3H), 1.31-1.36 (m, 2H), 1.40-1.46 (m, 2H), 1.57-1.64 (m, 2H), 1.74-1.80 (m, 2H), 2.27 (t,  $J=7.4$  Hz, 2H), 4.00 (t,  $J=6.9$  Hz, 2H), 4.12 (q,  $J=7.5$  Hz, 2H), 5.34 (s, 2H), 6.93-6.96 (m, 2H), 7.30-7.33 (m, 1H), 7.36 (dd,  $J=7.5, 7.5$  Hz, 2H), 7.40-7.45 (m, 3H), 7.81 (d,  $J=8.0$  Hz, 1H); ESI-TOF-HRMS ( $\text{M}+\text{Na}$ ) $^+$  calculated for  $\text{C}_{23}\text{H}_{28}\text{O}_5\text{Na}$  407.1829; found 407.1845.

**4.1.1.5. Benzyl 2-(8-ethoxy-8-oxooctyloxy)benzoate (1e)**

Colorless oil (54%):  $^1\text{H-NMR}$  (500 MHz,  $\text{CDCl}_3$ )  $\delta$  1.25 (t,  $J=7.5$  Hz, 3H), 1.28-1.34 (m, 4H), 1.37-1.45 (m, 2H), 1.58-1.64 (m, 2H), 1.74-1.78 (m, 2H), 2.27 (t,  $J=7.5$  Hz, 2H), 4.00 (t,  $J=6.9$  Hz, 2H), 4.12 (q,  $J=6.9$  Hz, 2H), 5.34 (s, 2H), 6.93-6.96 (m, 2H), 7.30-7.38 (m, 3H), 7.41-7.45 (m, 3H), 7.81 (d,  $J=8.0$  Hz, 1H); ESI-TOF-HRMS ( $\text{M}+\text{Na}$ ) $^+$  calculated for  $\text{C}_{24}\text{H}_{30}\text{O}_5\text{Na}$  421.1985; found 421.1995.

*General synthetic procedure for 2-(ethoxy-oxoalkyloxy)benzoic acids*

Palladium carbon (10 %) was added to a solution of the corresponding benzyl benzoate in EtOH. The mixture was stirred under a hydrogen atmosphere. After completion of the reaction, the mixture was filtered through a pad of celite. After removal of the solvent, the residue was purified by silica gel column chromatography (EtOAc/Hexane) to afford the product.

**4.1.1.6. 2-(4-ethoxy-4-oxobutyloxy)benzoic acid (2a)**

White solid (63 %):  $^1\text{H-NMR}$  (500 MHz,  $\text{CDCl}_3$ )  $\delta$  1.25 (t,  $J=7.5$  Hz, 3H), 2.21-2.27 (m, 2H), 2.53 (t,  $J=6.9$  Hz, 2H), 4.15 (q,  $J=7.4$  Hz, 2H), 4.32 (t,  $J=6.3$  Hz, 2H), 7.05 (d,  $J=7.5$  Hz, 1H), 7.13 (dd,  $J=7.5$ , 8.6 Hz, 1H), 7.55 (dd,  $J=7.5$ , 8.3 Hz, 1H), 8.18 (d,  $J=7.5$  Hz, 1H); ESI-TOF-HRMS ( $\text{M}+\text{Na}$ ) $^+$  calculated for  $\text{C}_{13}\text{H}_{16}\text{O}_5\text{Na}$  275.0890; found 275.0885.

**4.1.1.7. 2-(5-ethoxy-5-oxopentyloxy)benzoic acid (2b)**

Yellow oil (90 %):  $^1\text{H-NMR}$  (500 MHz,  $\text{CDCl}_3$ )  $\delta$  1.23 (t,  $J=6.9$  Hz, 3H), 1.78-1.84 (m, 2H), 1.92-1.97 (m, 2H), 2.39 (t,  $J=6.9$  Hz, 2H), 4.11 (q,  $J=7.5$  Hz, 2H), 4.24 (t,  $J=6.3$  Hz, 2H), 7.01 (d,  $J=8.0$  Hz, 1H), 7.10 (dd,  $J=7.5$ , 8.0 Hz, 1H), 7.52 (dd,  $J=6.9$ , 7.5 Hz, 1H), 8.14 (d,  $J=8.0$  Hz, 1H); ESI-TOF-HRMS ( $\text{M}+\text{Na}$ ) $^+$  calculated for  $\text{C}_{14}\text{H}_{18}\text{O}_5\text{Na}$  289.1046; found 289.1073.

**4.1.1.8. 2-(6-ethoxy-6-oxohexyloxy)benzoic acid (2c)**

Yellow solid (87 %):  $^1\text{H-NMR}$  (500 MHz,  $\text{CDCl}_3$ )  $\delta$  1.24 (t,  $J=6.9$  Hz, 3H), 1.50-1.56 (m, 2H), 1.68-1.74 (m, 2H), 1.92-1.95 (m, 2H), 2.33 (t,  $J=7.5$  Hz, 2H), 4.12 (q,  $J=6.9$  Hz, 2H), 4.25 (t,  $J=6.3$  Hz, 2H), 7.02 (d,  $J=8.0$  Hz, 1H), 7.11 (dd,  $J=7.5$ , 8.0 Hz, 1H), 7.53 (dd,  $J=7.5$ , 7.5 Hz, 1H), 8.16 (d,  $J=6.3$  Hz, 1H); ESI-TOF-HRMS ( $\text{M}-\text{H}$ ) $^+$  calculated for  $\text{C}_{15}\text{H}_{19}\text{O}_5$  279.1227; found 279.1229.

**4.1.1.9. 2-(7-ethoxy-7-oxooctyloxy)benzoic acid (2d)**

Yellow oil (99 %):  $^1\text{H-NMR}$  (500 MHz,  $\text{CDCl}_3$ )  $\delta$  1.24 (t,  $J=7.5$  Hz, 3H), 1.39-1.45 (m, 2H), 1.48-1.54 (m, 2H), 1.63-1.69 (m, 2H), 1.90-1.95 (m, 2H), 2.31 (t,  $J=7.5$  Hz, 2H), 4.12 (q,  $J=6.9$  Hz, 2H), 4.24 (t,  $J=6.9$  Hz, 2H), 7.03 (d,  $J=8.6$  Hz, 1H), 7.13 (d,  $J=6.9$ , 7.5 Hz, 1H), 7.54 (dd,  $J=7.5$ , 8.3 Hz, 1H), 8.18 (d,  $J=8.0$  Hz, 1H); ESI-TOF-HRMS ( $\text{M}+\text{Na}$ ) $^+$  calculated for  $\text{C}_{16}\text{H}_{22}\text{O}_5\text{Na}$  317.1359; found 317.1348.

**4.1.1.10. 2-(8-ethoxy-8-oxooctyloxy)benzoic acid (2e)**

Brown solid (92 %):  $^1\text{H-NMR}$  (500 MHz,  $\text{CDCl}_3$ )  $\delta$  1.24 (t,  $J=7.5$  Hz, 3H), 1.31-1.43 (m, 4H), 1.45-1.53 (m, 2H), 1.60-1.66 (m, 2H), 1.86-1.95 (m, 2H), 2.29 (t,  $J=6.9$  Hz, 2H), 4.11 (q,  $J=6.9$  Hz, 2H), 4.24 (t,  $J=6.3$  Hz, 2H), 7.03 (d,  $J=8.6$  Hz, 1H), 7.12 (d,  $J=7.4$ , 7.5 Hz, 1H), 7.54 (dd,  $J=7.5$ , 7.5 Hz, 1H), 8.17 (d,  $J=7.5$  Hz, 1H); ESI-TOF-HRMS ( $\text{M}-\text{H}$ ) $^+$

calculated for C<sub>17</sub>H<sub>23</sub>O<sub>5</sub> 307.1540; found 307.1543.

*General synthetic procedure for N<sup>6</sup>-benzoyl/heteroarylcarbonyladenine derivatives*

Benzoic acid or heteroaryl carboxylic acid (1.0 eq) and EDCI·HCl (1.2 eq) were added to a suspension of adenine (1.0 eq) in anhydrous DMA, and the mixture was stirred at 100°C-130 °C. After completion of the reaction, the solvent was removed under reduced pressure. The residue was purified by silica gel column chromatography (MeOH/CHCl<sub>3</sub>) and by washing with EtOAc and/or CH<sub>2</sub>Cl<sub>2</sub>/hexane (2:1 or 1:1 or 1:0) to afford the product.

**4.1.1.11. N<sup>6</sup>-[2-(4-Ethoxy-4-oxobutyloxy)benzoyl]adenine (3a)**

White solid (22 %): <sup>1</sup>H-NMR (500 MHz, DMSO-*d*<sub>6</sub>) δ 1.08 (t, *J*=6.9 Hz, 3H), 2.04-2.14 (m, 2H), 2.55 (t, *J*=7.5 Hz, 2H), 3.97 (q, *J*=6.9 Hz, 2H), 4.23 (t, *J*=6.3 Hz, 2H), 7.13 (dd, *J*=8.0, 8.1 Hz, 1H), 7.24 (d, *J*=8.0 Hz, 1H), 7.58 (dd, *J*=7.7, 8.0 Hz, 1H), 7.93 (d, *J*=7.5 Hz, 1H), 8.43 (s, 1H), 8.60 (s, 1H), 11.00 (s, 1H), 12.34 (brs, 1H); ESI-TOF-HRMS (M+Na)<sup>+</sup> calculated for C<sub>18</sub>H<sub>19</sub>N<sub>5</sub>O<sub>4</sub>Na 392.1329; found 392.1335.

**4.1.1.12. N<sup>6</sup>-[2-(5-Ethoxy-5-oxopentyloxy)benzoyl]adenine (3b)**

White solid (5 %): <sup>1</sup>H-NMR (500 MHz, CDCl<sub>3</sub>) δ 1.19 (t, *J*=7.5 Hz, 3H), 1.93-1.99 (m, 2H), 2.05-2.10 (m, 2H), 2.46 (t, *J*=7.5 Hz, 2H), 4.07 (q, *J*=7.5 Hz, 2H), 4.27 (t, *J*=6.3 Hz, 2H), 7.04 (d, *J*=8.1 Hz, 1H), 7.13 (dd, *J*=6.9, 8.0 Hz, 1H), 7.55 (dd, *J*=7.6, 7.9 Hz, 1H), 8.23 (d, *J*=8.1 Hz, 1H), 8.55 (s, 1H), 8.74 (s, 1H), 11.15 (brs, 1H); ESI-TOF-HRMS (M+Na)<sup>+</sup> calculated for C<sub>19</sub>H<sub>21</sub>N<sub>5</sub>O<sub>4</sub>Na 406.1486; found 406.1507.

**4.1.1.13. N<sup>6</sup>-[2-(6-Ethoxy-6-oxohexyloxy)benzoyl]adenine (3c)**

White solid (25 %): <sup>1</sup>H-NMR (500 MHz, DMSO-*d*<sub>6</sub>) δ 1.08 (t, *J*=7.5 Hz, 3H), 1.44-1.62 (m, 4H), 1.79-1.91 (m, 2H), 2.18-2.27 (m, 2H), 3.93 (q, *J*=7.5 Hz, 2H), 4.21 (t, *J*=6.3 Hz, 2H), 7.13 (dd, *J*=7.5, 8.0 Hz, 1H), 7.25 (d, *J*=8.0 Hz, 1H), 7.59 (dd, *J*=7.7, 7.8 Hz, 1H), 7.98 (d, *J*=8.0 Hz, 1H), 8.44 (s, 1H), 8.62 (s, 1H), 11.00 (brs, 1H), 12.32 (brs, 1H); ESI-TOF-HRMS (M+Na)<sup>+</sup> calculated for C<sub>20</sub>H<sub>23</sub>N<sub>5</sub>O<sub>4</sub>Na 420.1642; found 420.1659.

**4.1.1.14. N<sup>6</sup>-[2-(7-Ethoxy-7-oxoheptyloxy)benzoyl]adenine (3d)**

White solid (16 %): <sup>1</sup>H-NMR (500 MHz, CDCl<sub>3</sub>) δ 1.23 (t, *J*=7.5 Hz, 3H), 1.43-1.49 (m,

2H), 1.58-1.69 (m, 4H), 2.04-2.08 (m, 2H), 2.30 (t,  $J=7.5$  Hz, 2H), 4.11 (q,  $J=7.5$  Hz, 2H), 4.25-4.28 (m, 2H), 7.05 (d,  $J=8.1$  Hz, 1H), 7.11 (d,  $J=6.9, 7.5$  Hz, 1H), 7.57 (dd,  $J=6.9, 7.5$  Hz, 1H), 8.21 (d,  $J=7.5$  Hz, 1H), 9.11 (s, 1H), 9.57 (s, 1H), 11.63 (brs, 1H); ESI-TOF-HRMS (M+Na)<sup>+</sup> calculated for C<sub>21</sub>H<sub>25</sub>N<sub>5</sub>O<sub>4</sub>Na 434.1799; found 434.1788.

#### 4.1.1.15. *N*<sup>6</sup>-[2-(8-Ethoxy-8-oxooctyloxy)benzoyl]adenine (3e)

White solid (13 %): <sup>1</sup>H-NMR (500 MHz, DMSO-*d*<sub>6</sub>) δ 1.10 (t,  $J=6.9$  Hz, 3H), 1.15-1.23 (m, 2H), 1.24-1.36 (m, 2H), 1.37-1.54 (m, 4H), 1.79-1.90 (m, 2H), 2.17 (t,  $J=7.5$  Hz, 2H), 3.97 (q,  $J=6.9$  Hz, 2H), 4.21 (t,  $J=6.3$  Hz, 2H), 7.13 (dd,  $J=7.5, 7.5$  Hz, 1H), 7.26 (d,  $J=8.6$  Hz, 1H), 7.59 (dd,  $J=7.5, 8.0$  Hz, 1H), 7.98 (d,  $J=7.5$  Hz, 1H), 8.44 (s, 1H), 8.61 (s, 1H), 11.00 (brs, 1H), 12.33 (brs, 1H); ESI-TOF-HRMS (M+Na)<sup>+</sup> calculated for C<sub>22</sub>H<sub>27</sub>N<sub>5</sub>O<sub>4</sub>Na 448.1955; found 448.1983.

#### *General synthetic procedure for THP-protected hydroxamic acids*

1-Ethyl-3-(3-dimethylaminopropyl)carbodiimide hydrochloride (1.2 eq), 1-hydroxybenzotriazole monohydrate (1.2 eq) and *o*-(tetrahydropyran-2-yl)hydroxylamine (1.5 eq) were added to a solution of the corresponding carboxylic acid (1.0 eq) in DMF and the mixture was stirred at room temperature. After completion of the reaction, the solvent was removed under reduced pressure. The residue was purified by silica gel column chromatography (MeOH/CHCl<sub>3</sub>) to afford the product.

#### 4.1.1.16.

#### *N*<sup>6</sup>-(2-{4-[(tetrahydro-2*H*-pyran-2-yl)oxy]amino-4-oxobutyloxy}benzoyl)adenine (4a)

White solid (2 steps, 20 %): <sup>1</sup>H-NMR (500 MHz, CDCl<sub>3</sub>) δ 1.38-1.58 (m, 3H), 1.62-1.80 (m, 3H), 2.22-2.34 (m, 2H), 2.44-2.56 (m, 2H), 3.35-3.41 (m, 1H), 3.75-3.82 (m, 1H), 4.26 (t,  $J=5.2$  Hz, 2H), 4.87 (s, 1H), 7.02 (d,  $J=8.6$  Hz, 1H), 7.06 (dd,  $J=7.5, 8.0$  Hz, 1H), 7.50 (dd,  $J=7.7, 8.3$  Hz, 1H), 8.10 (d,  $J=7.5$  Hz, 1H), 8.43 (s, 1H), 8.72 (s, 1H); ESI-TOF-HRMS (M+Na)<sup>+</sup> calculated for C<sub>21</sub>H<sub>24</sub>N<sub>6</sub>O<sub>5</sub>Na 463.1700; found 463.1698.

#### 4.1.1.17.

#### *N*<sup>6</sup>-(2-{5-[(tetrahydro-2*H*-pyran-2-yl)oxy]amino-5-oxopentyloxy}benzoyl)adenine

**(4b)**

White solid (2 steps, 72 %):  $^1\text{H-NMR}$  (500 MHz,  $\text{CDCl}_3$ )  $\delta$  1.43-1.60 (m, 3H), 1.65-1.82 (m, 3H), 1.91-1.99 (m, 2H), 2.05-2.10 (m, 2H), 2.29 (t,  $J=6.3$  Hz, 2H), 3.51 (d,  $J=10.9$  Hz, 1H), 3.88 (t,  $J=9.7$  Hz, 1H), 4.23 (t,  $J=6.3$  Hz, 2H), 4.88 (s, 1H), 7.02 (d,  $J=8.6$  Hz, 1H), 7.09 (dd,  $J=7.5, 7.5$  Hz, 1H), 7.53 (dd,  $J=6.9, 7.5$  Hz, 1H), 8.18 (d,  $J=7.5$  Hz, 1H), 8.51 (brs, 1H), 8.73 (s, 1H); ESI-TOF-HRMS ( $\text{M}+\text{Na}$ ) $^+$  calculated for  $\text{C}_{22}\text{H}_{26}\text{N}_6\text{O}_5\text{Na}$  477.1857; found 477.1859.

**4.1.1.18.**

**$\text{N}^6$ -(2-{6-[(tetrahydro-2H-pyran-2-yl)oxy]amino-6-oxohexyloxy}benzoyl)adenine**

**(4c)**

White solid (2 steps, 87 %):  $^1\text{H-NMR}$  (500 MHz,  $\text{CDCl}_3$ )  $\delta$  1.45-1.79 (m, 10H), 1.99-2.07 (m, 2H), 2.13 (t,  $J=6.9$  Hz, 2H), 3.48-3.55 (m, 1H), 3.87-3.91 (m, 1H), 4.24 (t,  $J=6.3$  Hz, 2H), 4.85 (brs, 1H), 7.05 (d,  $J=8.0$  Hz, 1H), 7.12 (dd,  $J=6.9, 7.4$  Hz, 1H), 7.56 (dd,  $J=7.8, 8.3$  Hz, 1H), 8.22 (d,  $J=8.0$  Hz, 1H), 8.83 (s, 1H), 8.95 (s, 1H); ESI-TOF-HRMS ( $\text{M}+\text{Na}$ ) $^+$  calculated for  $\text{C}_{23}\text{H}_{28}\text{N}_6\text{O}_5\text{Na}$  491.2013; found 491.2042.

**4.1.1.19.**

**$\text{N}^6$ -(2-{7-[(tetrahydro-2H-pyran-2-yl)oxy]amino-7-oxoheptyloxy}benzoyl)adenine**

**(4d)**

White solid (2 steps, 54 %):  $^1\text{H-NMR}$  (500 MHz,  $\text{CDCl}_3$ )  $\delta$  1.46-1.77 (m, 12H), 2.00 (brs, 2H), 2.21 (brs, 2H), 3.56 (d,  $J=11.2$  Hz, 1H), 3.97 (brs, 1H), 4.16 (brs, 2H), 4.98 (brs, 1H), 6.97 (d,  $J=8.0$  Hz, 1H), 7.05 (brs, 1H), 7.49 (brs, 1H), 8.13 (d,  $J=6.9$  Hz, 1H), 8.66 (s, 1H), 8.77 (s, 1H), 9.75 (brs, 1H), 11.07 (brs, 1H); ESI-TOF-HRMS ( $\text{M}+\text{Na}$ ) $^+$  calculated for  $\text{C}_{24}\text{H}_{30}\text{N}_6\text{O}_5\text{Na}$  505.2170; found 505.2183.

**4.1.1.20.**

**$\text{N}^6$ -(2-{8-[(tetrahydro-2H-pyran-2-yl)oxy]amino-8-oxooctyloxy}benzoyl)adenine**

**(4e)**

White solid (2 steps, 49 %):  $^1\text{H-NMR}$  (500 MHz,  $\text{CDCl}_3$ )  $\delta$  1.26-1.36 (m, 2H), 1.36-1.46 (m, 2H), 1.47-1.84 (m, 10H), 1.92-2.14 (m, 2H), 2.05-2.17 (m, 2H), 3.53-3.60 (m, 1H), 3.85-4.02 (m, 1H), 4.02 (t,  $J=6.3$  Hz, 2H), 4.95 (s, 1H), 7.02 (d,  $J=8.0$  Hz, 1H), 7.09 (dd,  $J=7.5, 8.0$  Hz, 1H), 7.53 (dd,  $J=7.7, 8.3$  Hz, 1H), 8.20 (d,  $J=7.5$  Hz, 1H), 8.50 (s,

1H), 8.76 (s, 1H), 11.11 (s, 1H); ESI-TOF-HRMS (M+Na)<sup>+</sup> calculated for C<sub>25</sub>H<sub>32</sub>N<sub>6</sub>O<sub>5</sub>Na 519.2326; found 519.2330.

*General synthetic procedure for N<sup>6</sup>-[2-(hydroxyamino-oxoalkoxy)benzoyl]adenines*  
*p*-toluenesulfuric acid (0.4 eq) was added to a solution of the corresponding THP-protected hydroxamic acids (1.0 eq) in MeOH and the mixture was stirred at room temperature. After completion of the reaction, the solvent was removed under reduced pressure. The residue was purified by silica gel column chromatography (MeOH/CHCl<sub>3</sub>) to afford the product.

#### 4.1.1.21. N<sup>6</sup>-[2-(4-hydroxyamino-4-oxobutyloxy)benzoyl]adenine (5a)

White solid (24 %): m.p. 214.0-215.0 °C; <sup>1</sup>H-NMR (500 MHz, DMSO-*d*<sub>6</sub>) δ 2.03-2.12 (m, 2H), 2.20 (t, *J*=6.9 Hz, 2H), 4.20 (t, *J*=6.3 Hz, 2H), 7.14 (dd, *J*=7.5, 8.0 Hz, 1H), 7.24 (d, *J*=8.6 Hz, 1H), 7.59 (dd, *J*=6.9, 8.6 Hz, 1H), 7.96 (d, *J*=7.5 Hz, 1H), 8.45 (brs, 1H), 8.63 (s, 1H), 8.69 (brs, 1H), 10.34 (brs, 1H), 11.00 (brs, 1H), 12.34 (brs, 1H); ESI-TOF-HRMS (M-H)<sup>-</sup> calculated for C<sub>16</sub>H<sub>15</sub>N<sub>6</sub>O<sub>4</sub> 355.1149; found 355.1153.

#### 4.1.1.22. N<sup>6</sup>-[2-(5-hydroxyamino-5-oxopentyloxy)benzoyl]adenine (5b)

White solid (81 %): m.p. 168.0-169.0 °C; <sup>1</sup>H-NMR (500 MHz, DMSO-*d*<sub>6</sub>) δ 1.65-1.78 (m, 2H), 1.78-1.94 (m, 2H), 2.02 (t, *J*=6.9 Hz, 2H), 4.22 (t, *J*=6.3 Hz, 2H), 7.14 (dd, *J*=7.5, 7.5 Hz, 1H), 7.26 (d, *J*=8.0 Hz, 1H), 7.60 (dd, *J*=6.9, 8.6 Hz, 1H), 7.98 (d, *J*=8.0 Hz, 1H), 8.45 (s, 1H), 8.65 (brs, 2H), 10.33 (s, 1H), 11.04 (s, 1H), 12.33 (brs, 1H); ESI-TOF-HRMS (M-H)<sup>-</sup> calculated for C<sub>17</sub>H<sub>17</sub>N<sub>6</sub>O<sub>4</sub> 369.1306; found 369.1303.

#### 4.1.1.23. N<sup>6</sup>-[2-(6-hydroxyamino-6-oxohexyloxy)benzoyl]adenine (5c)

White solid (30 %): m.p. 193.0-194.0 °C; <sup>1</sup>H-NMR (500 MHz, DMSO-*d*<sub>6</sub>) δ 1.44-1.58 (m, 4H), 1.83-1.89 (m, 2H), 1.92 (t, *J*=6.8 Hz, 2H), 4.21 (t, *J*=6.3 Hz, 2H), 7.14 (dd, *J*=6.9, 7.5 Hz, 1H), 7.26 (d, *J*=8.6 Hz, 1H), 7.59 (dd, *J*=7.7, 7.7 Hz, 1H), 7.99 (d, *J*=8.0 Hz, 1H), 8.45 (s, 1H), 8.65 (brs, 2H), 10.31 (s, 1H), 11.02 (s, 1H), 12.34 (brs, 1H); ESI-TOF-HRMS (M-H)<sup>-</sup> calculated for C<sub>18</sub>H<sub>19</sub>N<sub>6</sub>O<sub>4</sub> 383.1462; found 383.1463.

#### 4.1.1.24. N<sup>6</sup>-[2-(7-hydroxyamino-7-oxoheptyloxy)benzoyl]adenine (5d)

White solid (36 %): m.p. 193.0-195.0 °C; <sup>1</sup>H-NMR (500 MHz, DMSO-*d*<sub>6</sub>) δ 1.26-1.32 (m, 2H), 1.44-1.51 (m, 4H), 1.83-1.86 (m, 2H), 1.89 (t, *J*=7.5 Hz, 2H), 4.22 (t, *J*=6.3 Hz, 2H), 7.14 (dd, *J*=8.0, 8.0 Hz, 1H), 7.26 (d, *J*=8.6 Hz, 1H), 7.60 (dd, *J*=7.7, 7.8 Hz, 1H), 8.00 (d, *J*=8.1 Hz, 1H), 8.45 (s, 1H), 8.65 (s, 1H), 10.29 (brs, 1H), 11.01 (brs, 1H), 12.38 (brs, 1H); ESI-TOF-HRMS (M+Na)<sup>+</sup> calculated for C<sub>19</sub>H<sub>22</sub>N<sub>6</sub>O<sub>4</sub>Na 421.1595; found 421.1614.

#### 4.1.1.25. *N*<sup>6</sup>-[2-(8-hydroxyamino-8-oxooctyloxy)benzoyl]adenine (5e)

White solid (64 %): m.p. 155.0-157.0 °C; <sup>1</sup>H-NMR (500 MHz, CD<sub>3</sub>OD) δ 1.28-1.35 (m, 2H), 1.41-1.47 (m, 2H), 1.56-1.64 (m, 4H), 1.97-2.01 (m, 2H), 2.04 (t, *J*=7.5 Hz, 2H), 4.29 (t, *J*=6.3 Hz, 2H), 7.14 (dd, *J*=7.4, 8.1 Hz, 1H), 7.23 (d, *J*=8.6 Hz, 1H), 7.60 (dd, *J*=7.8, 8.0 Hz, 1H), 8.21 (d, *J*=8.0 Hz, 1H), 8.49 (s, 1H), 8.64 (s, 1H); ESI-TOF-HRMS (M-H)<sup>-</sup> calculated for C<sub>20</sub>H<sub>23</sub>N<sub>6</sub>O<sub>4</sub> 411.1775; found 411.1752.

## 4.2 BRD4 bromodomain1 TR-FRET assay

BRD4-inhibitory activity was evaluated by means of europium-based LANCE TR-FRET (time-resolved fluorescence resonance energy transfer) assay using a BRD4 bromodomain 1 TR-FRET assay kit (No. 600520, Cayman). (+)-JQ1 (No. 11187, Cayman) was used as a positive control. Plates were read in the time-resolved format with excitation at 320 nm and emission at 615 and 665 nm, using a 100 μs delay and a 400 μs reading window on an Envision (PerkinElmer). Data analysis was performed using the TR-FRET ratio (665 nm emission/615 nm emission).

## 4.3 Fluor de Lys®-Green HDAC Assay

HDAC-inhibitory activity was evaluated using a Fluor de Lys®-Green HDAC assay kit (BML-AK530, Enzo Life Sciences). SAHA (No. 10009929, Cayman) was used as a positive control. Plates were read with excitation at 485 nm and emission at 535 nm on an Envision (PerkinElmer).

## 4.4 Cell culture

HL-60 cells, K-562 cells, OVCAR-5 cells, A2780 cells, and T-47D cells were cultured in

RPMI 1640 supplemented with 10 % FBS and penicillin/streptomycin mixture, and MCF-7 cells were cultured in D-MEM (High Glucose) supplemented with 10 % FBS and penicillin/streptomycin mixture at 37 °C in a humidified incubator (5 % CO<sub>2</sub> in air).

#### **4.5 HL-60 cells or K-562 cells growth-inhibiting activity assay**

HL-60 cells or K-562 cells were seeded at a density of  $1 \times 10^5$  cells/mL in 24-well plates and treated with test compounds or DMSO. After incubation for 3 days, the living cells were counted.

#### **4.6 Annexin V assay**

HL-60 cells were seeded at a density of  $4 \times 10^5$  cells/mL (0 h or 24 h), or  $1 \times 10^5$  cells/mL (48 h) in 24-well plates and treated with test compounds or DMSO. After incubation for 0 h, 24 h, or 48 h, the cells were suspended in 1×binding buffer [Annexin V-FITC Apoptosis Detection Kit, BioVision (No. K101-100)] at a density of  $1 \times 10^6$  cells/mL, and then Annexin V-FITC and PI were added according to the supplier's protocol. After incubation for 5 min at room temperature, the cells were analyzed by flow cytometry using BD FACSCanto™II.

#### **4.7 Western blot analysis**

Cell lysates were boiled in SDS sample buffer at 100 °C for 5 min and then cooled on ice for 10 min, and subjected to SDS-PAGE using SuperSep™ Ace 5-12% or 10-20%. The proteins were transferred to PVDF membrane. After blocking with 5% skim milk, the membrane was probed with the primary antibody (anti-PARP, anti-caspase 3, or anti- $\alpha$ -tubulin) and washed three times with TBS-T buffer. Then, the membrane was probed with appropriate secondary antibody (anti-rabbit or anti-mouse) and washed three times with TBS-T buffer. The immunoblots were visualized by enhanced chemiluminescence with Immobilon™ Western Chemiluminescent HRP substrate.

#### **4.8 HL-60 cell differentiation-inducing activity assay**

HL-60 cells were seeded at a density of  $1 \times 10^5$  cells/mL in 24-well plates and treated with test compounds or DMSO. After incubation for 1 h, the cells were treated with ATRA or DMSO and incubated for 3 days. PBS containing 0.2 % NBT and 20 nM TPA in a 1:1

(v/v) ratio was added, and incubation was continued at 37 °C for 30 min. NBT-positive cells were counted. After Wright-Giemsa staining, cell differentiation was morphologically evaluated by microscopy.

#### 4.9 c-MYC production-inhibiting activity assay

HL-60 cells were seeded at a density of  $5 \times 10^5$  cells/mL in 60 mm dishes and treated with test compounds or DMSO. After incubation for 24 h, the cells were lysed with lysis buffer at a density of  $4 \times 10^6$  cells/mL and sonicated using a Bioruptor®, Diagnode. The c-MYC levels were measured by using Human c-MYC (Total) ELISA kit (No. KH02041, Enzo Life Technologies) according to the supplier's protocol.

#### 4.10 WST-1 assay

OVCAR-5 cells or T-47D cells were seeded at a density of  $5 \times 10^4$  cells/mL, and A2780 cells or MCF-7 cells were seeded at a density of  $2 \times 10^4$  cells/mL respectively. After incubation for 1 day, the cells were treated with test compounds or DMSO. After incubation for 3 days, cell growth-inhibitory activity was determined by using WST-1 [Cell Counting Kit, Dojindo (No. CK01)], according to the supplier's protocol.

#### Acknowledgements

The work described in this paper was partially supported by Grants-in-Aid for Scientific Research from The Ministry of Education, Culture, Sports, Science and Technology, Japan, and a grant from The Japan Society for the Promotion of Science. We are grateful to Dr. Yuki Okada for the sonication device, Bioruptor®, and to Dr. Yutaka Enomoto, and Dr. Eiko Saijyo-Oikawa for their help with flow-cytometric detection.

#### References and notes

1. A.L. Hopkins. *Nat. Chem. Biol.*, 4(11), 682-90 (2008).
2. A.L. Hopkins, J. S. Mason, J. P. Overington. *Curr. Opin. Struct. Biol.*, 16(1), 127-36 (2006).
3. M. L. Bolognesi. *Curr. Med. Chem.*, 20 (13), 1639-45 (2013).

4. T. Noguchi-Yachide, T. Sakai, Y. Hashimoto, T. Yamaguchi. *Bioorg. Med. Chem.*, 23, 953-9 (2015).
5. S. Amemiya, T. Yamaguchi, T. Sakai, H. Hashimoto, T. Noguchi-Yachide. *Chem., Pharm. Bull.* 64, 1378-1383 (2016).
6. M. K. Jang, K. Mochizuki, M. Zhou, H. S. Jeong, J. N. Brady, K. Ozato. *Mol. Cell.*, 19(4), 523-34 (2005).
7. S. Rahman, M. E. Sowa, M. Ottinger, J. A. Smith, Y. Shi, J. W. Harper, P. M. Howley. *Mol Cell Biol.*, 31(13), 2641-52 (2011).
8. R. Taube, X. Lin, D. Irwin, K. Fujinaga, B. M. Peterlin. *Mol. Cell. Biol.*, 22, 321-31 (2002).
9. J. Lovén, H. A. Hoke, C. Y. Lin, A. Lau, D. A. Orlando, C. R. Vakoc, J. E. Bradner, T. I. Lee, R. A. Young. *Cell*, 153, 320-34 (2013).
10. T. Kanno, Y. Kanno, G. LeRoy, E. Campos, H. W. Sun, S. R. Brooks, G. Vahedi, T. D. Heightman, B. A. Garcia, D. Reinberg, U. Siebenlist, J. J. O'Shea, K. Ozato. *Nat. Struct. Mol. Biol.*, 21, 1047-57 (2014).
11. D. S. Hewings, T. P. Rooney, L. E. Jennings, D. A. Hay, C. J. Schofield, P. E. Brennan, S. Knapp, S. J. Conway. *J. Med. Chem.*, 55(22), 9393-413 (2012).
12. T. Noguchi-Yachide, *Chem. Pharm. Bull.*, 64, 540-7 (2016).
13. S. J. Conway, *ACS Med. Chem. Lett.*, 3(9), 691-694 (2012).
14. A. J. de Ruijter, A. H. van Gennip, H. N. Caron, S. Kemp, A. B. van Kuilenburg. *Biochem. J.*, 370, 737-49(2003).
15. M. Heberland, R. L. Montgomery, E. N. Olson. *Nat. Rev. Genet.*, 10, 32-42 (2009).
16. P. P. Pandolfi. *Cancer Chemother. Pharmacol.*, 48 (Suppl. 1), S17-9 (2001).
17. R. J. Lin, T. Sternsdorf, M. Tini, R. M. Evans. *Oncogene*, 20, 7204-15 (2001).
18. J. E. Bolden, M. J. Peart, R. W. Johnstone. *Nat. Rev. Drug Discov.*, 5, 769-84 (2006).
19. C. Zwergel, S. Valente, C. Jacob, A. Mai. *Expert Opin. Drug Discov.*, 10, 599-613 (2015).
20. J. Bhadury, L. M. Nilsson, S. V. Muralidharan, L. C. Green, Z. Li, E. M. Gesner, H. C. Hansen, U. B. Keller, K. G. McLure, J. A. Nilsson. *Proc. Natl. Acad. Sci U S A.*, 111(26): E2721-30 (2014).
21. S. Picaud, M. Strocchia, S. Terracciano, G. Lauro, J. Mendez, D. L. Daniels, R. Riccio, G. Bifulco, I. Bruno, P. Filippakopoulos, *J. Med. Chem.*, 58, 2718-36

- (2015).
22. K. J. Falkenberg, R. W. Johnstone. *Nat. Rev. Drug Discov.* 13, 673-91 (2014).
  23. Z. Yang, N. He, Q. Zhou. *Mol. Cell. Biol.* 28(3), 967-76 (2008).
  24. K. Mochizuki, A. Nishiyama, M. K. Jang, A. Dey, A. Ghosh, T. Tamura, H. Natsume, H. Yao, K. Ozato. *J. Biol. Chem.* 283(14), 9040-8 (2008).
  25. J. Zuber, J. Shi, E. Wang, A. R. Rappaport, H. Herrmann, E. A. Sison, D. Magoon, J. Qi, K. Blatt, M. Wunderlich, M. J. Taylor, C. Johns, A. Chicas, J. C. Mulloy, S.C. Kogan, P. Brown, P. Valent, J. E. Bradner, S. W. Lowe, C. R. Vakoc. *Nature.* 478(7370), 524-8 (2011).
  26. J. A. Mertz, A. R. Conery, B. M. Bryant, P. Sandy, S. Balasubramanian, D. A. Mele, L. Bergeron, R. J. 3rd. Sims. *Proc. Nat.l Acad. Sci. U S A.* 108(40), 16669-74 (2011).
  27. P. Filippakopoulos, S. Knapp. *Nat Rev Drug Discov.* 13(5), 337-56 (2014).
  28. M. A. Gluzak, E. Seto. *Oncogene.* 26, 5420-32 (2007).
  29. S. Roper, M. Esteller. *Mol Oncol.* 1(1), 19-25 (2007).
  30. K. J. Falkenberg, R. W. Johnstone. *Nat. Rev. Drug Discov.* 13, 673-91 (2014).
  31. M. Haberland, R. L. Montgomery, E. N. Olson. *Nat. Rev. Genet.* 10(1), 32-42 (2009).
  32. P. Rathert, M. Roth, T. Neumann, F. Muerdter, J. S. Roe, M. Muhar, S. Deswal, S. Cerny-Reiterer, B. Peter, J. Jude, T. Hoffmann, Ł. M. Boryń, E. Axelsson, N. Schweifer, U. Tontsch-Grunt, L. E. Dow, D. Gianni, M. Pearson, P. Valent, A. Stark, N. Kraut, C. R. Vakoc, J. Zuber. *Nature.* 525(7570), 543-7 (2015).
  33. S. Shu, C. Y. Lin, H. H. He, R. M. Witwicki, D. P. Tabassum, J. M. Roberts, M. Janiszewska, S. J. Huh, Y. Liang, J. Ryan, E. Doherty, H. Mohammed, H. Guo, D. G. Stover, M. B. Ekram, G. Peluffo, J. Brown, C. D'Santos, I. E. Krop, D. Dillon, M. McKeown, C. Ott, J. Qi, M. Ni, P. K. Rao, M. Duarte, S. Y. Wu, C. M. Chiang, L. Anders, R. A. Young, E. P. Winer, A. Letai, W. T. Barry, J. S. Carroll, H. W. Long, M. Brown, X. S. Liu, C. A. Meyer, J. E. Bradner, K. Polyak. *Nature.* 529(7586), 413-7 (2016).
  34. A. M. Kurimchak, C. Shelton, K. E. Duncan, K. J. Johnson, J. Brown, S. O'Brien, R. Gabbasov, L. S. Fink, Y. Li, N. Lounsbury, M. Abou-Gharbia, W. E. Childers, D. C. Connolly, J. Chernoff, J. R. Peterson, J. S. Duncan. *Cell Rep.* 16(5), 1273-86 (2016).